INTERNATIONAL JOURNAL OF OPTIMIZATION IN CIVIL ENGINEERING
Int. J. Optim. Civil Eng., 2017; 7(3):339-354

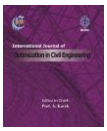

OPTIMAL DESIGN OF TUNNEL SUPPORT LINING USING MCBO ALGORITHM

H. Fazli[*, †]
Department of Civil Engineering, Payame Noor University, Tehran, Iran

ABSTRACT

In this paper, a systematic approach is presented for optimal design of tunnel support lining using two-dimensional finite element analysis models of soil-structure interaction developed in ABAQUS software and the Modified Colliding Bodies Optimization (MCBO) algorithm implemented in MATLAB environment. This approach is then employed to study the influence of variable geometrical and geo-mechanical parameters on the optimal design of a class of practical access tunnels.

Keywords: optimization; access tunnel; tunnel support; MPSO; ABAQUS; MATLAB.

Received: 20 October 2016; Accepted: 27 January 2017

1. INTRODUCTION

Development of subway transportation in urban areas involves the construction of so many underground spaces. Such spaces may differ in structural form, construction method and functional aspects, and may include but not limited to railway tunnels, metro stations, 3-way intersections, tunnel bifurcations, crossovers, cross passages, ventilation or access shafts and access tunnels or galleries. Access tunnels, simply called Galleries, as implied in this text, are referred to those tunnels with small cross sectional area and limited length intended for the transit of passengers or circulation of fresh air. These galleries are commonly constructed using a Sequential Construction Method (SCM) also known as New Austrian Tunneling Method (NATM). In this method the ground is excavated in multiple rounds and an initial support is provided early on. In soft ground and weak rock the installation of support directly follows the excavation of a round length and prior to proceeding to the excavation of the next round in sequence. The initial support mainly consists of a shotcrete lining of thickness ranging from 100 to 400 mm, reinforced with a single layer or two layers of steel wire mesh. Three-dimensional steel frames fabricated from lattice girders or rolled

[*]Corresponding author: Department of Civil Engineering, Payame Noor University, Tehran, Iran
[†]E-mail address: hfazli@alumni.iust.ac.ir (H. Fazli)

steel shapes are generally integrated into the shotcrete lining. The regular cross section of the tunnel generally consists of an arch roof; straight side walls and a flat invert (see Fig. 1). Although this is not an optimal geometry to promote smooth stress distribution around the tunnel opening, it is most often employed for economy reasons. The oval or curvilinear cross sections require accommodation of modular formworks for the construction of final cast in place concrete lining, which is costly for tunnels with varying small cross sections and short lengths.

Traditionally, the process of designing tunnel support lining involves a rough determination of design variables based on experience and intuition. This may often lead to controversial and economically unfavorable designs. Hence, the development of some standard methods for producing optimal designs would have practical significance. The subject of tunnel support optimization has been treated from different perspectives in the past. These include topology optimization [1-4], shape optimization [5], and multi-objective optimization [6], to name a few.

In this paper, the main objective is to develop a systematic approach toward optimal design of tunnel support lining using an efficient finite element analysis and an advanced optimization algorithm. For the first time the Modified Colliding Bodies Optimization (MCBO) algorithm has been applied to tunnel support design optimization problem. This approach is then employed to study the influence of variable geometrical and geo-mechanical parameters on the optimal design of a class of practical access tunnels.

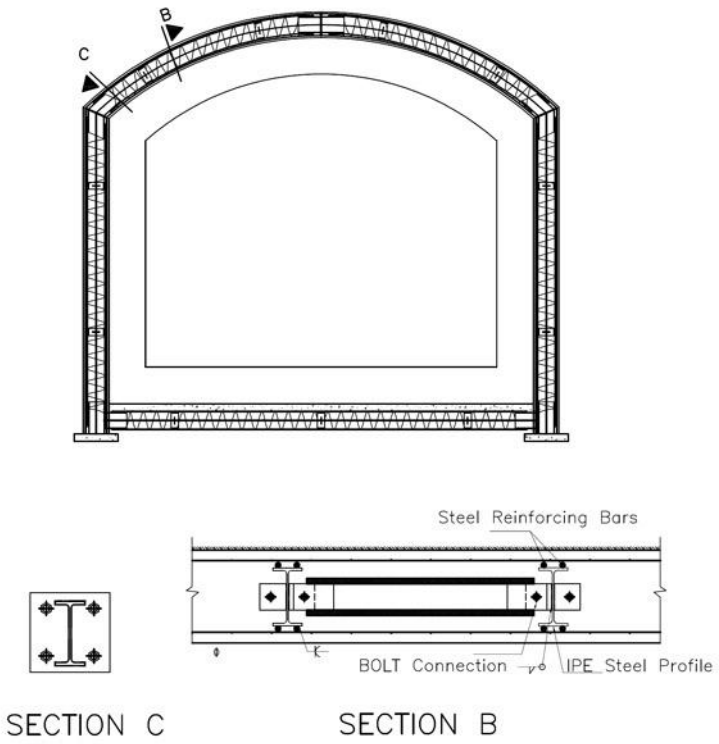

Figure 1. Typical cross section of access tunnels

2. TUNNEL SUPPORT DESIGN OPTIMIZATION

2.1 Modeling and analysis of tunnel

Tunnel support system considered in this research for design optimization, consists of lattice girder frames and sprayed concrete. For the analysis of soil-support interaction, two-dimensional finite element models are developed in general purpose finite element program ABAQUS [7]. The software is adopted not only because of its superior performance in solving complex structural analysis problems, but more importantly due to its intrinsic features that facilitate input/output communications with other programming applications. This latter property makes the software apt to be incorporated into optimization codes developed in programming environments such as MATLAB [8].

Simulation of staged construction of tunnels with ABAQUS requires special modeling and analysis techniques to be employed. The three-dimensional arching effect is accounted for by using the convergence-confinement method [9], also called the load reduction method or β-method [10]. In this method, the analysis starts from initial geostatic stress field due to gravitational and tectonic forces. This field varies linearly through the depth of the soil and the ratio between the horizontal and vertical stress components is assumed as $K_0 = 1 - \sin\varphi$, where φ is the angle of friction of the soil.

The excavation of the tunnel is accomplished by applying the forces that are required to maintain equilibrium with the initial stress state in the surrounding material as loads p_0 on the perimeter of the tunnel. The stress relaxation of the ground due to the delayed installation of the shotcrete lining is modeled by reducing these loads down to $\beta.p_0$, with $0 < \beta < 1$. At this stage, the lining is installed and the remaining load $\beta.p_0$ is divided over the lining and the ground. Fig. 2 illustrates these calculation phases by relating them to the so-called ground-response curve.

The β-value, simply referred to as the unloading factor, is an 'experience value' and depends on many factors such as excavation round length, ground stiffness, soil strength parameters, coefficient of lateral earth pressure at rest and tunnel depth. Another important point is that one needs to use different β-values in order to compute both structural forces and settlements precisely. In this research, recommendations given in [11] for selecting suitable β values are followed.

In summary, soil excavation and installation of tunnel support is modeled in four analysis steps as follows:

- **First step**: the initial stress state is applied and the support elements are removed using the *MODEL CHANGE, REMOVE option. Concentrated loads p_0 are applied on the perimeter of the tunnel. These forces are obtained from an independent initial stress field analysis where the displacements on the tunnel perimeter were constrained.
- **Second step**: tunnel excavation begins by reducing the concentrated loads on the tunnel surface down to $\beta.p_0$.
- **Third step**: tunnel support is installed using the *MODEL CHANGE, ADD option. No deformation takes place in the soil or support during the third step.

– **Fourth step**: excavation is completed by removing the remainder of the load on the tunnel perimeter.

Fig. 3 depicts a typical numerical model of an access tunnel created in ABAQUS software. Due to symmetry, half the tunnel is simulated.

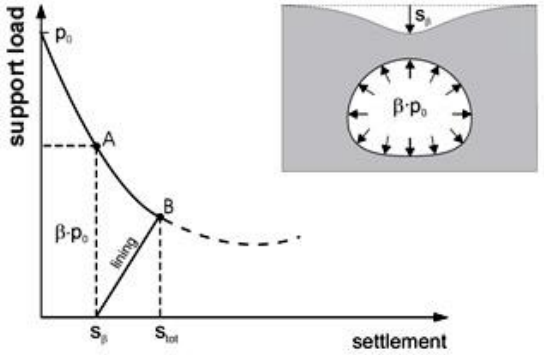

Figure 2. Load reduction method adopting ground response curve by Addenbrooke et al. (1997) [12]

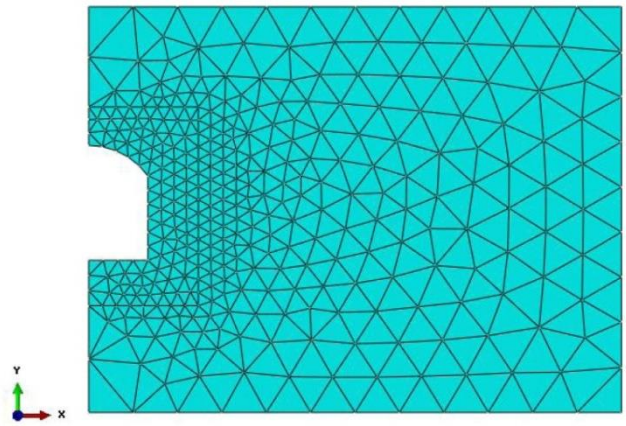

Figure 3. A typical numerical model of access tunnel

2.2 Design variables

A set of design variables defines a design solution, which has to satisfy some design constraints in order to be feasible. At this point, an evaluation and optimization process can be carried out. The structural design of initial lining is governed by three design variables namely *r*, *t* and *d*: *r* being the round length or frame spacing along the tunnel axis, *t*: shotcrete thickness and *d*: steel reinforcement diameter.

2.3 Objective function

The objective function is based on minimum tunnel support cost. This includes material plus labor, overhead and waste for two main items i.e. concrete and reinforcement. Different feasible designs are compared for their relative initial cost per unit area of tunnel support.

$$C_T(t,d,r) = C_c + C_s \tag{1}$$

where

$C_T(t,d,r)$: total cost of tunnel support per unit area which is a function of shotcrete thickness *t*, round length *r* and rebar diameter *d* for specified tunnel dimensions.

$C_c(t)$: cost of sprayed concrete per unit area, which is a function of shotcrete thickness.

$C_s(d,r)$: cost of reinforcement per unite area of tunnel support, which is a function of round length and rebar diameter.

In this research, the cost items are compiled from approved national bill of quantities for works and materials. For comparison purposes, cost functions are normalized such that the lowest price design is represented with a unit cost.

2.4 Constraints

Two groups of constraints have been considered; physical-geometrical constraints and safety constraints.

2.4.1 Physical-geometrical constraints

Round length or longitudinal Frame spacing is limited to the range [500, 1750] mm, with increments of 250 mm.

$$\begin{cases} r \geq 500mm \\ r \leq 1750mm \\ r = 500 + 250n,\ n = 1,2,... \end{cases} \tag{2}$$

Shotcrete thickness is limited in the range [100, 400] mm, with 50 mm increments.

$$\begin{cases} t \geq 100mm \\ t \leq 400mm \\ t = 100 + 50n,\ n = 1,2,... \end{cases} \tag{3}$$

Longitudinal steel reinforcement of lattice girders is restricted to the following bar diameters

$$d \in \{18, 20, 22, 25, 28, 32\}\ mm \tag{4}$$

2.4.2 Safety constraints

Safety constraints are subdivided into three categories: ground surface settlement, tunnel support strength, and tunnel heading stability.

Ground surface settlement

Estimation of tunneling induced settlements at the ground surface is of great concern due to its potential impact on the settlement behavior of any overlying or adjacent bridge foundations, building structures, or buried utilities transverse or parallel to the alignment of the proposed tunnel excavation. Empirical data and numerical analyses suggest the shape of the settlement trough typically approximates the shape of an inverse Gaussian curve (Fig. 4).

Evaluation of structural tolerance to settlement requires definition of the possible damage that a structure might experience. A number of methods for evaluating the impact of settlements on building or other facilities have been proposed and used. Wahls [13] proposed a correlation between angular distortion (the relative settlement between columns or measurement points) and building damage category. As an alternative initial screening method, Rankin [14] proposed a damage risk assessment chart based on maximum building slope and settlement as shown in Table 1.

In this paper, risk category 2 is selected based on the Rankin's method, restricting the maximum ground surface settlement and maximum slope to 20 mm and 1/500, respectively.

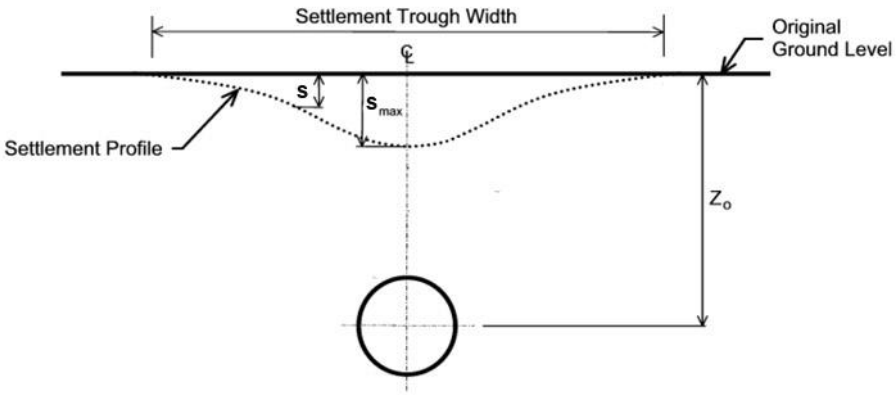

Figure 4. Typical Settlement Profile for a soft ground tunneling

Table 1: Damage risk assessment chart (Rankin)

Risk category	Maximum slope of building	Maximum settlement of building (mm)	Description of risk
1	< 1/500	< 10	Negligible: superficial damage unlikely
2	1/500 – 1/200	10 - 50	Slight: possible superficial damage which is unlikely to have structural significance
3	1/200 – 1/50	50 - 75	Moderate: expected superficial damage and possible structural damage to buildings, possible damage to relatively rigid pipelines
4	> 1/50	> 75	High: expected structural damage to buildings. Expected damage to rigid pipelines, possible damage to other pipelines

Tunnel support strength

The structural capacity of the initial linings is evaluated using so called Capacity Limit Curves or "CLCs." The calculated section force combinations N-M, are mapped onto these CLCs charts to evaluate the adequacy of the structural lining section.

Section force combinations N-M are obtained from each finite element included in the representation of the lining in the numerical modeling. These forces are magnified using load combinations of ACI 318 [15]. The lining is modeled using elastic plate elements with axial and flexural rigidities computed based on shotcrete lining specifications. Flexural rigidity of the lining is reduced by a factor 0.5 to account for the effects of concrete cracking. The capacity of the lining is computed in accordance with ACI 318 considering lining thickness, shotcrete design strength, and structural reinforcement of the lining section.

Design of shotcrete is based on its early-stage compressive strength specified as $f_c^{'} = 15\,\text{MPa}$ For the reinforcement, deformed bars with tensile yield strength of $f_y = 400\,\text{MPa}$ are used.

Tunnel heading stability

The stability of tunnel face or heading can be analyzed on the basis of sliding wedge mechanism or by using a 3-D finite element analysis. However, such an analysis is dropped in this research since it is assumed that the sequencing of the excavation can be adjusted such that the heading stability is assured by subdividing the tunnel cross section into multiple drifts as needed. The only implication of such an assumption is the right choice of unloading or β-values in the 2-D analyses.

2.5 Solution of optimal design problem

The optimal design problem is highly nonlinear due to nonlinearity of cost function and constrains. Furthermore the inter-dependence between analysis results and design variables increases the nonlinearity of the problem. It is well-known that the solution of large nonlinear optimization problems using mathematical programming methods becomes inefficient due to a large number of gradient calculations. Therefore, an extensive research effort has been devoted to developing powerful algorithms in order to find the global optimum in an affordable time without being entrapped in local optima. Meta-heuristic algorithms [16, 17] such as Genetic algorithms (GA) [18], Particle swarm optimization (PSO) [19], Ant colony optimization (ACO) [20], Big bang-big crunch (BB-BC) [21], Charged system search (CSS) [22], Ray optimization (RO) [23], Dolphin echolocation (DE) [24], Colliding Bodies Optimization (CBO) [25], are now well established and successfully applied to different structural optimization problems. Recently, Kaveh and co-authors [26] applied a modified version of Colliding Bodies Optimization denoted by MCBO to optimize the cost of post-tensioned concrete box girder bridge superstructures and demonstrated the efficiency and robustness of the MCBO algorithm. In this paper this method of optimization is adapted for tunnel support design, due to its superior performance and ease of implementation.

2.5.1 Background of the CBO algorithm

The CBO algorithm proposed by Kaveh and Mahdavi [25] is a population-based algorithm for optimization problems. This algorithm takes its inspiration from the physic laws. In physics, collisions between bodies are governed by two laws, the law of momentum and energy. When a collision occurs in an isolated system (Fig. 5), the total momentum and energy of the system of objects is conserved. Using the conservation of the total momentum and total kinetic energy, the velocities after a one-dimensional collision can be obtained as:

$$v_1^{'} = \frac{(m_1 - \varepsilon m_2)v_1 + (m_2 + \varepsilon m_2)v_2}{m_1 + m_2} \tag{5}$$

$$v_2^{'} = \frac{(m_2 - \varepsilon m_1)v_2 + (m_1 + \varepsilon m_1)v_1}{m_1 + m_2} \tag{6}$$

where v_1 and v_2 are the initial velocity of the first and second objects before impact, also $v_1^{'}$ and $v_2^{'}$ are the final velocity of the first and second objects after impact, respectively. m_1 and m_2 are the mass of the first and second objects. ε is the coefficient of restitution (COR) of two colliding bodies, defined as the ratio of relative velocity of separation to relative velocity of approach:

$$\varepsilon = \frac{\left|v_2^{'} - v_1^{'}\right|}{\left|v_2 - v_1\right|} \tag{7}$$

According to the coefficient of restitution, two special cases of collision can be considered as:

1. A perfectly elastic collision is defined as the one in which there is no loss of kinetic energy in the collision ($\varepsilon = 1$). In reality, any macroscopic collision between objects will convert some kinetic energy to internal energy and other forms of energy. In this case, after collision the velocity of separation is high.
2. An inelastic collision is the one in which part of the kinetic energy is changed to some other form of energy in the collision. Momentum is conserved in inelastic collisions (as it is for elastic collisions), but one cannot track the kinetic energy through the collision since some of it is converted to other forms of energy. In this case, coefficient of restitution does not equal unity ($\varepsilon \leq 1$). Here, after collision the velocity of separation is low. For most of the real objects, ε is between 0 and 1.

2.5.2 The CBO algorithm

In this algorithm each solution candidate is considered as a colliding body (CB). All of the CBs are divided equally into stationary and moving objects. An inelastic collision occurs between pairs of objects in which the moving objects move to follow stationary objects. The two purposes of this collision are to improve the position of moving objects and to push stationary objects toward better positions. After the collision, the new positions of the

colliding bodies are updated based on the new velocity using the collision law discussed in the previous section. The CBO procedure can briefly be outlined as follow:

Step 1. The initial positions of the CBs are randomly determined using a uniform distribution.

Step 2. The magnitude of the body mass for each CB (in minimization problems) is defined as:

$$m_i = \frac{1/fit(i)}{\sum_{k=1}^{N} 1/fit(k)} \quad i = 1,...,N \tag{8}$$

where *fit(i)* represents the objective function value of the *i*th CB and *N* is the population size taken as 200 in this paper.

Step 3. The CBs are sorted based on their body mass, and equally divided into two groups. The upper half of the CBs are good agents which are stationary and their velocities before collision are zero. The lower half of CBs (the moving group) move toward the upper half. The best CBs of the both groups will collide together and similarly the worst CBs of both groups will collide each other. The difference of the position of CBs represents these bodies' velocities before collision.

Step 4. After the collisions, velocities of bodies in each group are evaluated using Eqs. (5) and (6). The velocity of each stationary and moving CBs after the collision is:

$$v_i' = \frac{(m_{i+\frac{N}{2}} + \varepsilon m_{i+\frac{N}{2}})v_{i+\frac{N}{2}}}{m_i + m_{i+\frac{N}{2}}}, \quad i = 1,...,\frac{N}{2} \tag{9}$$

$$v_i' = \frac{(m_i - \varepsilon m_{i-\frac{N}{2}})v_i}{m_i + m_{i-\frac{N}{2}}}, \quad i = 1,...,\frac{N}{2} \tag{10}$$

the coefficient of restitution ε is expressed in this paper as:

$$\varepsilon = 1 - \frac{iter}{iter_{\max}} \tag{11}$$

where *iter* is the current iteration number, and $iter_{\max}$ is the maximum number of iterations.

Step 5. The new position of each CBs is:

$$X_i^{new} = X_i + \text{rand} \circ v_i', \quad i = 1,...,\frac{N}{2} \tag{12}$$

$$X_i^{new} = X_{i-\frac{N}{2}} + \text{rand} \circ v_i', \quad i = \frac{N}{2}+1,...,N \tag{13}$$

where X_i^{new} is the new position of *i*th CB after the collision. rand is a random vector uniformly distributed in the range (−1 , 1) and the sign ' '∘' ' denotes an element – by - element multiplication.

Step 6. The optimization is repeated from Step 2 until a termination criterion is satisfied

2.5.3 The modified CBO algorithm

In the standard version of the CBO algorithm the positions of all CBs are changed after collision in each iteration. Therefore, in the next iterations, the algorithm would lose the effect of the best solutions that the algorithm has found so far. Although changing the position of the best solutions can improve the diversification of search process, it reduces the intensification. Therefore, the algorithm is not able to efficiently follow the best solutions. In order to avoid this shortcoming, we do not change the position of a specific number of the best CBs. These CBs are saved in a memory to be used in the next iterations. In addition, in order to control the exploitation and exploration of the algorithm we define a constant parameter (α) and use a nonlinear function for defining the coefficient of restitution:

$$\varepsilon = e^{-\alpha \frac{iter}{iter_{\max}}} \tag{14}$$

The value of parameter α is selected based on the type of a problem and could be varied from 2 to 10. In Fig. 6 the variation of function ε versus iteration number is shown for different values of α. By increasing the value of α the nonlinearity of the function increases. In this paper, we consider the value of α equal to 4.

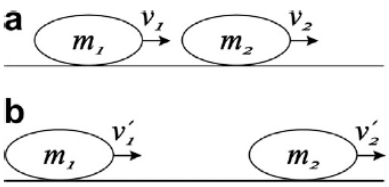

Figure 5. Collision between two bodies. (a) before collision, (b) after collision

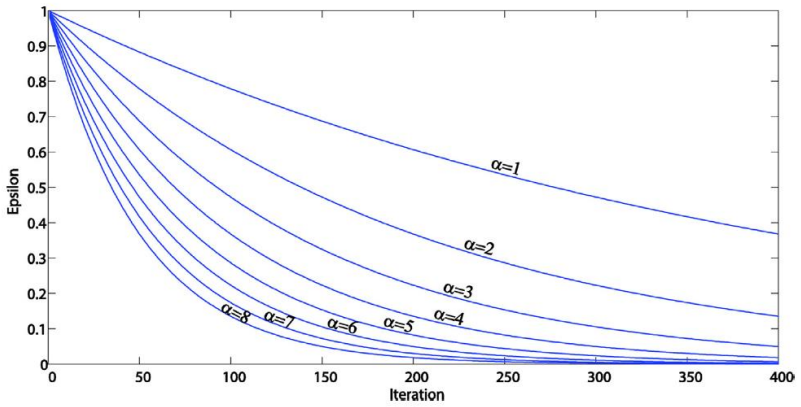

Figure 6. variation of restitution function with iteration number for different values of α

3. OPTIMAL DESIGN OF TUNNEL SUPPORT- PRACTICAL APPLICATION

3.1 Investigation outline

To achieve the stated objectives of the investigation, the above mentioned optimization procedure has been used to produce optimal tunnel support design for a variety of access tunnels constructed in soft ground.

As stated in section 2.2, design variables include shotcrete thickness, bar diameter for lattice girders and excavation round length (longitudinal spacing between lattice frames). The effect of varying main parameters influencing optimal support designs are studied. These include geometric parameters of tunnel (i.e. tunnel span length, sidewall height and overburden depth) and geotechnical parameters of the soil.

3.1.1 Tunnel geometric parameters

Fig. 7 shows the geometric information of the tunnels investigated here. Five span lengths are considered: S = 3, 4, 5, 6, 7 m. The wall height h is taken as 3 and 4 m for span lengths S = 3 & 4 m and S = 5 to 7 m, respectively. The overburden depth is considered to be H = 4 to 20 m.

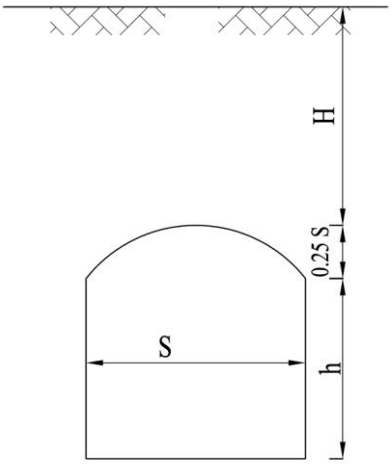

Figurre 7. Geometric parameters of investigated tunnels

3.1.2 Geotechnical parameters

The well-known Mohr-Coulomb model is used in this research for characterizing the constitutive behavior of soils. The Mohr-Coulomb model is an elastic perfectly-plastic model with a fixed yield surface, i.e. the yield surface is fully defined by model parameters and is not affected by (plastic) straining. It requires five basic input parameters, namely a stiffness parameter or Young's modulus, E, a Poisson's ratio, ν, two strength parameters including cohesion, c, and friction angle, φ, and a dilatancy angle, ψ. For sands and near normally consolidated clays subjected to loading, the secant modulus at 50% strength denoted as E_{50} is used as Young's modulus.

Soils commonly encountered in urban tunneling are a mix of multiple layers of soft to hard clay, sandy clay, loose or dense sand, silty sand or sandy gravel, with diverse stiffness and strength parameters. Note that both E_{50} as the basic stiffness modulus, and c as the shear strength parameter, tend to increase with the confining pressure, hence, in reality, deep soil layers tend to have greater stiffness and cohesion than shallow layers. In order to keep it simple, it is preferred in this research to stick to single average global parameters of stiffness and strength for entire soil medium. This modeling strategy has the advantage that more general conclusions may be drawn by letting global soil parameters to vary over an admissible range.

Table 2 presents the range of parameter values for analysis of tunnels by Mohr-Coulomb model.

Table 2: Soil parameter values (range of values)

Parameter		Unit	Value (Range Of Values)
Density	γ	kN/m^2	20
Modulus of elasticity	E	(MPa)	20-120
Poison's ratio	ν		0.2
Cohesion	c	(kPa)	5-100
Friction angle	φ	($^\circ$)	20-40
Dilation angle	ψ	($^\circ$)	0

3.2 The results of the present study

Optimal support designs are obtained for different overburden heights and span lengths and a set of selected average soil parameters. As stated before, design variables include shotcrete thickness, reinforcement diameter of 4-bar lattice frames and spacing between lattice frames. Soil medium is represented as a uniform layer with average geotechnical parameters stipulated in Table 2. The lower bound of the parameter ranges are selected which are representative of a relatively soft and weak Soil. Fig. 8 shows the cost per unit area of support versus overburden height (H) for different span lengths (S). The cost values are normalized such that the minimum value be equal to unity. For every H-S point, the optimum design is indicated by a 3-component expression "t-Φ-d". For example the expression "t30Φ28@1m" indicates a design with shotcerete thickness 30 cm, rebar diameter 28 mm and frame spacing of 1 m.

For specified tunnel geometry, the optimum design is obtained when shotcrete thickness and bar diameter are minimized and round length is maximized. Increasing the round length has two conflicting effects on the soil and structure performance: on the one hand, it reduces the loads applied to support structure due to more stress relaxation, and on the other hand, it results in increased settlements and even may cause heading instabilities. A balanced state is found by the optimization algorithm in which all the benefits are realized and at the same time the constraints are established.

Referring to Fig. 8 it can be claimed that for shallow to medium depth tunnels in loose ground, a round length of about 1 m is optimum. For deep tunnels, the spacing should be

reduced to 0.5 m. It is also inferred that the cost increases with increasing overburden height for all span lengths. However, the cost difference between the short and long spans is less remarkable for deeper tunnels. It is mainly due to the fact that in larger depths the design is governed by the forces developed in tunnel walls (the height of which is not so much dependent on the span length) rather than its arch roof.

In order to investigate the effect of soil stiffness or shear strength on the optimal solutions, a series of studies has been performed with different values of elastic modulus and cohesion in the admissible ranges stipulated in Table 2. The most severe span length of 7 m is selected for the analyses. The results of optimization are presented in Figs. 9 and 10 for soil parameters *E* and *c*, respectively. The optimal design labels are only depicted for two smallest and largest overburden heights. Examining these figures, the following remarks can be made:

- The cost of support construction per unit area increases by increasing the tunnel depth.
- For specified tunnel depth, the cost decreases with increasing soil stiffness or shear strength.
- In shallow tunnels, the improved soil parameters do not introduce a remarkable impact on tunnel support cost, as can be noticed from the slight slope of the charts depicted in lower portion of the plots. Increasing the soil stiffness, the round length is fixed to 1 m, however it is increased to 1.5 m for much cohesive soils. It can be inferred that cohesion is more responsible for settlement control than the soil stiffness in shallow tunnels, however none of them have a significant role in reducing the forces applied to the structure.
- For deeper tunnels, the effect of improved soil parameters is much better realized in cutting tunnel support cost. However, the cost drop is more remarkable for soil stiffness improvement, rather than it's shear strength, as can be inferred from the steeper chart of Fig. 9 compared to that of Fig. 10. It is indicated that increasing the soil stiffness not only reduces structural forces in deep tunnels, but also definitely restricts surface settlements such that the round lengths could be increased.

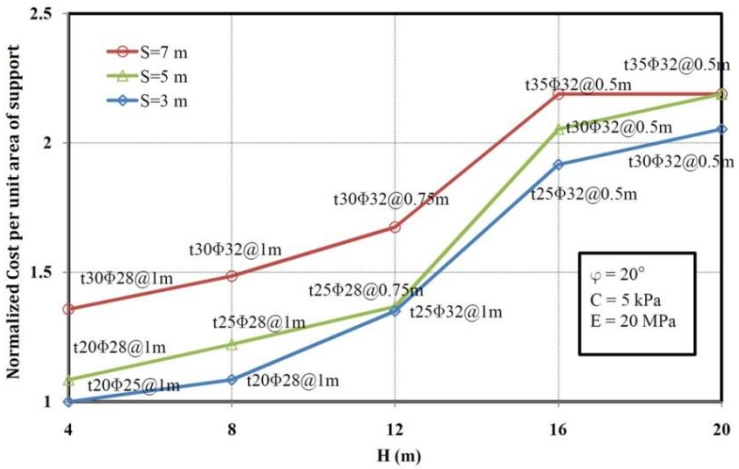

Figure 8. Results of optimal tunnel support design for different tunnel geometric dimensions

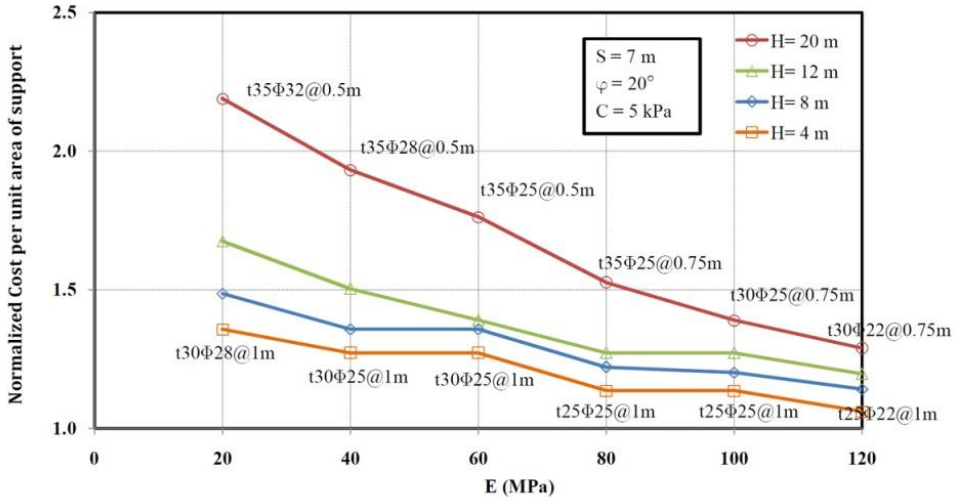

Figure 9. Results of optimal tunnel support design for varying soil stiffness

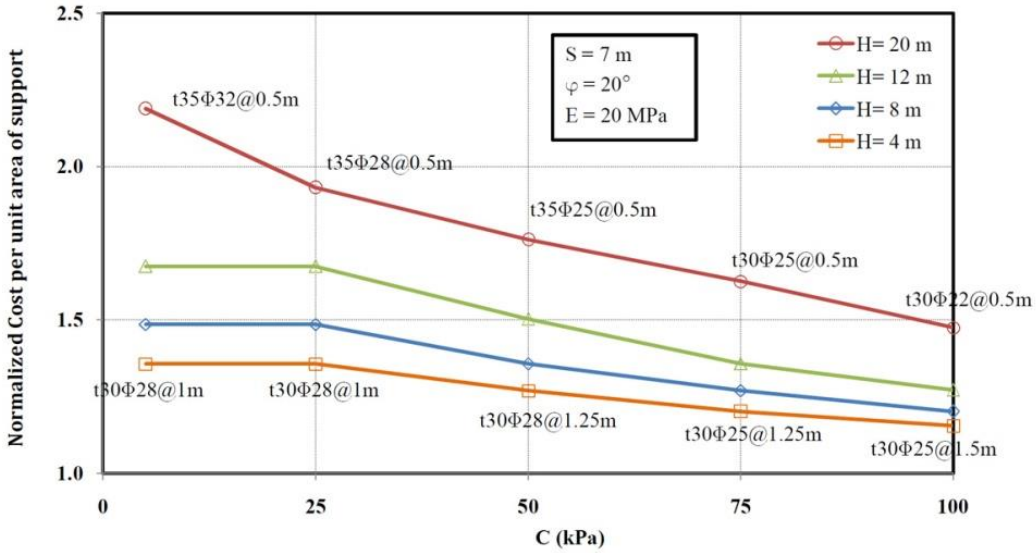

Figure 10. Results of optimal tunnel support design for varying shear strength

4. CONCLUSION

In this paper, an optimization approach is presented for the design of tunnel support lining structure. Due to complexity of the problem especially with regard to selection of the round length, the application of a meta-heuristic algorithm namely modified colliding bodies optimization (MCBO) is pursued. An implementation of the algorithm in Matlab environment is conducted to facilitate the incorporation of analysis results from soil-support interaction models developed in finite element analysis software ABAQUS.

Using the optimization approach developed here, optimal designs are obtained for a class

of practical access tunnels with different span lengths and overburden heights. The influence of soil stiffness and shear strength parameters on the optimal designs are also investigated. Based on the findings of this study, the following conclusions can be drawn:

- Optimization techniques can be effectively applied to tunnel support lining design, thus aiding the designer to produce more cost effective solutions.
- Selection of the excavation round length is a critical step in tunnel design which explicitly affects other important elements such as surface settlement and structural forces. Optimal values of 1 m and 0.5 m in loose ground are suggested by the optimization procedure for shallow and deep tunnels, respectively.
- Construction costs are reduced as soil stiffness and shear strength improve. The benefits are however more considerable for deep tunnels than shallow ones. The designs are also more favorably affected by increments of soil stiffness in comparison to shear strength.

Acknowledgements: The author would like to gratefully acknowledge department of transportation, metro and urban development of Mahab Ghodss consulting engineering company, especially Mr Jabarouti for inspiring the idea and also providing access to their invaluable directory of design documents.

REFERENCES

1. Liu Y, Jin F. Bi-direction evolutionary structural optimization Method for topology optimization of tunnel support, *Eng Mech* 2006; **23**: 110-5.
2. Yin L, Yang W. Topology optimization for tunnel support in layered geological structures, *Int J Numer Meth Eng* 2000; **47**: 1983-96.
3. Yin L, Yang W, Guo T. Tunnel reinforcement via topology optimization, *Int J Numer Analyt Meth Geomech* 2000; **24**: 201-13.
4. Nguyen T, Ghabraie K, Tran-Cong T. Applying bi-directional evolutionary structural optimisation method for tunnel reinforcement design considering nonlinear material behavior, *Comput Geotech* 2014; **55**: 57-66.
5. Ghabraie K, Xie YM, Huang X, Ren G. Shape and reinforcement optimization of underground tunnels, *J Comput Sci Technol* 2010; **4**: 51-63.
6. Tonon F, Mammino A, Bernardini A. Multiobjective optimization under uncertainty in tunneling: application to the design of tunnel support/reinforcement with case histories, *Tunnell Underground Space Technol* 2002; **17**: 33-54.
7. Hibbett, Karlsson, Sorensen. ABAQUS/standard: User's Manual: Hibbitt, Karlsson & Sorensen, 1998.
8. The mathworks Inc. N, MA. MATLAB User's Guide, 1998.
9. Panet M, Guenot A. Analysis of convergence behind the face of a tunnel, *Tunnelling, Proceedings of the 3rd International Symposium*, Brighton, 7–11 June 1982; **82**: pp. 197-204.
10. Möller S, Vermeer P. On numerical simulation of tunnel installation, *Tunnell Underground Space Technol* 2008; **23**: 461-75.
11. Möller SC. *Tunnel Induced Settlements and Structural Forces in Linings*, Universität Stuttgart, Institut für Geotechnik, 2006.

12. Addenbrooke T, Potts D, Puzrin A. The influence of pre-failure soil stiffness on the numerical analysis of tunnel construction, *Géotechnique* 1997; **47**: 693-712.
13. Wahls HE. Tolerable settlement of buildings, *J Geotech Eng, ASCE* 1981; **107**: 1489-504.
14. Rankin WJ. Ground movements resulting from urban tunnelling: Predictions and effects, *Geological Society London Engineering Geology Special Publications* 1988; **5**: 79-92.
15. ACI. Building code requirements for structural concrete (ACI 318-08) and commentary. American Concrete Institute, 2008.
16. Kaveh A. *Advances in Metaheuristic Algorithms for Optimal Design of Structures*, Switzerland: Springer International Publishing, 2017.
17. Kaveh A. *Applications of Metaheuristic Optimization Algorithms in Civil Engineering*, Switzerland, Springer, 2017.
18. Goldberg DE, Holland JH. Genetic algorithms and machine learning, *Mach Learn* 1988; **3**: 95-9.
19. Eberhart RC, Kennedy J. A new optimizer using particle swarm theory, *Proceedings of the Sixth International Symposium on Micro Machine and Human Science*, New York, NY, 1995. pp. 39-43.
20. Dorigo M, Maniezzo V, Colorni A. Ant system: optimization by a colony of cooperating agents, *IEEE Transact on Syst Man Cybernetics, Part B (Cybernetics)* 1996; **26**: 29-41.
21. Erol OK, Eksin I. A new optimization method: big bang–big crunch, *Adv Eng Softw* 2006; **37**: 106-11.
22. Kaveh A, Talatahari S. A novel heuristic optimization method: charged system search, *Acta Mech* 2010; **213**: 267-89.
23. Kaveh A, Khayatazad M. A new meta-heuristic method: ray optimization, *Comput Struct* 2012; **112**: 283-94.
24. Kaveh A, Farhoudi N. A new optimization method: Dolphin echolocation, *Adv Eng Softw* 2013; **59**: 53-70.
25. Kaveh A, Mahdavi V. Colliding bodies optimization: a novel meta-heuristic method, *Comput Struct* 2014; **139**: 18-27.
26. Kaveh A, Maniat M, Naeini MA. Cost optimum design of post-tensioned concrete bridges using a modified colliding bodies optimization algorithm, *Adv Eng Softw* 2016; **98**: 12-22.